Durability of bond between concrete beams and FRP composites made of flax and glass fibers

Article *in* Construction and Building Materials · November 2016

DOI: 10.1016/j.conbuildmat.2016.09.095

3 authors, including:

Pedram Sadeghian
Dalhousie University
23 PUBLICATIONS **66** CITATIONS

SEE PROFILE

DURABILITY OF BOND BETWEEN CONCRETE BEAMS AND FRP COMPOSITES MADE OF FLAX AND GLASS FIBERS

Laura Wroblewski [1], Dimo Hristozov [1], and Pedram Sadeghian [2]

[1] *School of Science, Engineering and Technology, Penn State Harrisburg University, 777 W. Harrisburg Pike, Middletown, Middletown, PA 17057, USA*

[2] *Department of Civil and Resource Engineering, Dalhousie University, 1360 Barrington Street, Halifax, NS, B3H 4R2, Canada. Email: Pedram.Sadeghian@dal.ca (corresponding author)*

ABSTRACT:

In this paper, the durability of flax and glass fiber-reinforced polymer (FRP) composites externally bonded to concrete beams is studied. A total of 100 plain concrete beam specimens (75 mm × 100 mm × 400 mm) were prepared and bonded with flax and glass FRP strips to the tension side of the beams. The specimens were designed to have an adhesive debonding failure of the FRP from the concrete. The specimens were aged in water and dry heat conditions at 20 and 60 °C for 21, 42, and 63 days and then were tested under three-point bending. A set of specimens were also aged by freeze/thaw cycles. The load-deflection behaviors of the specimens were evaluated and the effects of heat, moisture, and freeze/thaw cycles on the peak load and ductility of the specimens were quantified. The study shows that the peak load retentions of the specimens with bonded flax and glass FRPs immersed in 60 °C water for 63 days is 72% and 80% of their counterparts kept in dry heat condition, respectively. An analysis of variance was also performed to assess the significance of the aging effects on the physical and mechanical properties of the specimens. Also, a cross-sectional analytical modeling was performed to compute the FRP tensile force, strain, and bond strength of the specimens.

KEYWORDS: composite; polymer; flax; glass; concrete; durability; bond.

1. INTRODUCTION

During the past three decades, synthetic fibers such as glass and carbon fibers have been widely applied for the repair and strengthening of existing concrete structures in the form of externally bonded fiber-reinforced polymer (FRP) composites [1-2]. Synthetic fibers are made of non-renewable resources and their production typically emits significant greenhouse gases contributing to the global warming. Moreover, it is very difficult to recycle FRP composites made of synthetic fibers (hereafter called synthetic FRPs) at the end of their life span. As a result, synthetic FRPs are typically sent to landfills that are filling up fast [3-4]. Natural fibres extracted from plants (e.g. flax, hemp, jute, and etc.) are good examples of renewable materials that offer several economical, technical, and ecological advantages over synthetic fibres. FRP composites made of natural fibers (hereafter called natural FRPs) have a potential at the end of their life span for recycling and degradation, depending on the type of the polymer used. The worst case scenario is the incineration of natural FRPs to generate power, which reduces their volume significantly to fly ash and bottom ash with many potential applications in concrete industry.

Natural FRPs have been extensively researched for the past two decades [5-10]. Due to the relative large quantity, low cost of raw material, low density, high specific properties, and positive environmental profile; natural fibres are considered as prospective substitutes to synthetic fibres. Natural fibers have shown comparable mechanical properties to glass fibres. Despite of the positive characteristics, natural fibres have some negative characteristics. They are highly hydrophilic and their mechanical and physical properties are dependent on the climate, location, and weather; so it is difficult to predict their respective composite properties and failure mechanism [11-14]. In terms of long-term performance of natural FRPs, there are drawbacks with respect to their durability against moisture and other environmental conditions [15-18].

On the other hand, the durability of synthetic FRPs externally bonded to concrete structures have been extensively studied [19-28]. It has been shown that the bond between FRP and concrete can be deteriorated by aging and exposure to environmental conditions. Many parameters including material properties, type of environmental exposure, type of loading, and quality of workmanship can affect the deterioration of the bond [29]. It is already known that the bond between glass FRPs and concrete can be deteriorated by exposing to harsh environmental condition. However, the mechanism of bond deterioration has not been completely characterized, as FRP materials are relatively new compared to traditional construction materials. Consequently, long-term field data are limited, making the use of accelerated durability tests essential in the field. However, due to lack of standard protocols for conducting accelerated durability testing, it has been difficult to draw detailed conclusions from the large database of test results generated over the past two decades [30]. In addition, there is no data regarding the bond between concrete and natural FRPs. As natural fibers are more sensitive than synthetic fibers to moisture, the durability of the bond between natural FRPs and concrete also needs to be studied in-depth.

In this study, accelerated durability tests were conducted in order to investigate the long-term behavior of both synthetic (glass) and natural (flax) FRPs externally bonded to concrete beams. A total of 100 plain concrete beams were prepared. The specimens were externally bonded with flax and glass fabrics using a vinyl ester resin. The test specimens were aged for 21, 42, and 63 days in water and dry heat at 20 and 60 °C and then were tested under three-point bending and their mechanical properties were compared to control specimens. The weight gain of the specimens and the pH and temperature of the solutions were also observed. The load-deflection behavior of the specimens were evaluated and the effect of heat, moisture, and freeze/thaw cycles on the strength and ductility of the specimens were studied. Also, the peak load retention of the specimens immersed in

water with respect to their counterparts kept in dry heat condition were evaluated. At the end, a cross-sectional analytical modeling was performed to compute the tensile force and strain the FRPs as well as to evaluate the bond strength between the FRP and concrete of the experimental specimens.

2. EXPERIMENTAL PROGRAM

The experimental program implemented in this study follows the overall concept of the accelerated conditioning protocol (ACP) recommended by ACI 440.9R-15 [30] for FRP-bonded concrete beams. However, the size of specimens, exposure duration, and width of bonded FRPs differ from the ACP. The size of compartments in freeze/thaw cabinet, time limitation of the study, and low strength of flax FRPs controlled the specific changes. The critical mechanism is considered to be the effect of moisture accelerated by heat on the aging of the bond between FRP and concrete. After the aging process, the FRP-bonded beams are tested under a three-point bending set-up using the method developed by Gartner et al. [31]. An adhesive bond failure mode is typically expected, which is where the fracture surface passes entirely through the FRP-concrete interface, not in the concrete (i.e. cohesive failure). This is important to evaluate the durability of the FRP-concrete interface bond (i.e., adhesive bond failure mode). It should be mentioned that some mortar particles from the concrete may remain adhered to the FRP when adhesive bond failure occurs [30]. In order to prevent FRP rupture failure mode, the width of the flax FRP is selected wider than the test method developed by Gartner et al. [31] and recommended by ACI 440.9R-15 [30]. The width of glass FRP is accordingly selected as same as the flax FRP to make the bond area the same. In addition to the properties of the polymer adhesive, the durability of the FRP-concrete interface is a function of concrete surface preparation, mechanical interlock, and chemical interactions between the adherents. It also could be a function of the type of fibers and fiber content. The permeable nature of natural fibres comparing to

synthetic fibers can create more moisture path into the polymer leading to higher moisture absorption [32-35] and consequently more bond deterioration. This is why both flax and glass fibers were considered in this experimental study. The sections below provide a detailed description of the test matrix, material properties, specimen fabrication, environmental conditioning, and test setup of the experimental program.

2.1. Test Matrix

A total of 100 plain concrete beams (75 mm × 100 mm × 400 mm) were prepared. After concrete moisture curing, the specimens were bonded with flax and glass fabrics using a vinyl-ester resin. The test parameters are: fiber type (flax vs. glass fibers), aging condition (dry heat, immersion in water, and freeze/thaw), exposure duration (21, 42, and 63 days), and temperature during the exposure (20 and 60 °C). For each case, five identical specimens were prepared as shown in Table 1. The test specimens are identified with the specimen identification (ID) as F-X-TY-DZ and G-X-TY-DZ, where F stands for flax FRP, and G stands for glass FRP. In addition, X stands for the environmental exposure of air day (AD), water (W), and freeze/thaw (FT); Y stands for the exposure temperature of 20 °C (T20) and 60 °C (T60); and Z stands for the exposure duration of 21 days (D21), 42 days (D42), and 63 days (D63). For example, F-W-T60-D63 is a beam with bonded flax FRP immersed in 60 °C water for 63 days and G-AD-T20-D63 is a beam with bonded glass FRP kept in 20 °C air dry condition for 63 days. The specimens identified as F-FT-C25 and G-FT-C25 are exposed to 25 cycles of freeze/thaw. Also, control specimens are identified by D0.

2.2. Material Properties

All specimens were constructed from similar concrete mix design as shown in Table 2. The cement used was Portland cement type I/II and coarse aggregate used had a maximum size of 19 mm. It should be mentioned that all aggregates larger than 19 mm were removed by the corresponding sieve. Per ACI 318-11 [36], the nominal maximum size of coarse aggregate shall be not larger than 1/5 the narrowest dimension between sides of forms (i.e., 75/5=15 mm), however the limitation shall not apply, if the judgment of the professional, workability, and method of consolidation are such that concrete can be placed without voids. As a table shaker was used for concrete consolidation and the result was satisfactory, the maximum coarse aggregate size of 19 mm was selected. As an adhesive bond failure is targeted, the aggregate size has no significant effect. The compressive strength of concrete was determined by testing three cylinders (100 mm × 200 mm) resulted in an average compressive strength of 45 MPa right after 28-day moisture curing. At the time of testing of the control FRP-bonded beams, three more cylinders were tested and resulted in an average compressive strength of 49 MPa. Also, at the time of testing the 63-day aged FRP-bonded beams, three more cylinders were tested and resulted in an average compressive strength of 55 MPa.

For making flax FRPs, two layers of a 275 gsm (g/m^2) stitched unidirectional flax fabric was used. The fabric was made of flax fibers with the single fiber density of 1.4-1.5 g/cm^3, diameter of 20 μm, tensile strength of 500-900 MPa, elastic modulus of 50-70 GPa, and rupture strain of 2% reported by manufacturer (Composite Evolution, Chesterfield, UK). For making glass FRPs, one layer of a 955 gsm stitched unidirectional glass fabric was used (manufacturer: Fibre Glast, Brookville, OH, USA). For making both flax and glass FRPs, a vinyl-ester resin was used and catalyzed with 1.25% methyl ethyl ketone peroxide (MEKP) by weight. The resin (cured at room temperature for 24 hours

and post-cured for 2 hours at 138 °C) had the tensile strength of 82 MPa, elastic modulus 3720 MPa, and rupture strain of 7.9% reported by manufacturer (Fibre Glast, Brookville, OH, USA).

Five identical coupons of flax and glass FRPs were also prepared and tested in tension [37]. The load-strain response of the coupons was monitored with an extensometer, then the stiffness of the materials per unit width and the ultimate tensile strain of the materials was determined based on ASTM D7565 [38]. Specimen thickness is not required for the calculations. Fig. 1 shows the load-strain response results of flax and glass FRP coupons. The average maximum tensile force per unit width of flax and glass FRPs was 207±10 and 649±31 N/mm, respectively. The plus and minus range shows a standard deviation. The dashed lines in Fig. 1 show the initial tensile stiffness per unit width, of flax and glass FRPs with the average values of 21.9 ±1.3 and 28.0±1.0 kN/mm, respectively. As shown in the figure, the glass FRPs have almost a linear behavior up to the rupture, however flax FRPs exhibit a bilinear behavior with a transition zone at a strain ranging from 0.002 to 0.003 mm/mm and a secondary stiffness of almost two-third of the initial stiffness. The non-linear behavior may affect the behavior and failure mode of concrete specimens with bonded flax FRPs as it will be discussed later.

2.3. Specimen Fabrication

As shown in Fig. 2, the concrete was poured into custom-made wooden forms with five cells in each panel to make 75 mm × 100 mm × 400 mm plain concrete beams. The size of the specimens were selected based on the size of compartments in freeze/thaw cabinet. After keeping under plastic sheets for 24 hours, the wooden forms were removed and the concrete beams were set in a curing room with 100% relative humidity up to the age of 28 days. After the moisture curing was completed, the beam specimens were saw cut on a form finished face at mid-span to a depth of 50 mm (i.e., half of the 100

mm side was saw cut) to ensure that a single bending crack is made at the tip of the saw cut [31]. The 3 mm wide saw cut provided two identical development lengths for the bonded FRP from the beam mid-span as shown in Fig. 3. In order to enhance the bonding of concrete and FRP, the same concrete surface was roughened with a concrete surface grinder to reach a minimum concrete surface profile (CSP) 3 according to ACI 440.2R-08 [39]. Then, the specimens were dried for a period of 48 hours in an air circulating oven at a temperature of 50 °C.

After a minimum 5 hours cooling at room temperature, the roughened surface of concrete was coated with the resin and immediately flax/glass fabric impregnated by the resin was applied on the wet surface. One layer of glass fabric or two layers of flax fabrics (75 mm wide × 200 mm long) were used as the density of the glass fabric was higher. It was ensured that the fabrics were impregnated properly and excessive resin was removed from the surface by a roller. It should be noted that most of the researchers used 25-50 mm wide glass/carbon FRP strips [29-31], however in this research the FRPs bonded over the full width of the beams. This was necessary to avoid the rupture failure mode of flax FRPs, as they are much weaker than glass/carbon FRPs. For comparison purpose, the width and length of both flax and glass FRPs were selected the same. Moreover, due to the lower tensile strength of flax FRP, two layers of flax fabrics were used to ensure the bond failure occurs rather than the tensile rupture.

After FRPs cured for 7 days at room temperature, the specimens were pre-conditioned for a period of 48 hours in an air circulating oven at a temperature of 50 °C, because the specific resin used in this study showed lack of full curing at room temperature [35]. The purpose of the pre-conditioning was to ensure the resin was cured completely. The authors are aware that this pre-conditioning regimen is not possible in the field. However, as the same pre-conditioning was used for both flax and glass FRP bonded specimens, their performances can be compared. The pre-conditioning was

also used to dry the specimens before the aging process. The weight of the specimens at dry condition was obtained to monitor the weight gain (i.e. moisture absorption) of the specimens after the aging process. It should be noted that the majority of weight gain during the aging is due to water absorbed by the concrete, however the weight gain can be larger for the specimen with bonded flax FRPs. This information will be useful later for comparison of flax and glass FRPs. After weighing, the specimens were ready to be aged in different environmental conditions.

2.4. Environmental Conditioning

The beam specimens with bonded FRPs were immersed into containers filled with tap water. The containers were kept at two different temperatures, namely room temperature and 60 °C air circulating oven as presented in Table 1. The aging temperature of 60 °C was selected per ACI 440.9R-15 [30]. As the glass transition temperature of the resin was not reported and the authors did not have access to required equipment to find the glass transition temperature, it was ensured that the aging temperature was well below the heat distortion temperature (98 °C) of the resin provided by manufacturer. The containers were sealed to control evaporation. In addition, similar specimens were kept in an air dry condition in oven and room temperature for comparison. For room temperature cases, the air dry specimens were kept on a dry shelf and the rest of specimens were immersed into water containers kept in an air conditioned room. The mechanical tests were conducted at 21, 42, and 63 days (i.e. 500, 1000, and 1500 hours) after the environmental conditionings started. Initially, longer exposure durations were targeted, but due to time limitation of the project, the maximum duration of 63 days was selected. For each case, five identical specimens were prepared and tested. At the time intervals (i.e. when the containers were opened to take some specimens out for the mechanical testing), the specimens were taken out of water, their surfaces were made dried using a paper towel

and immediately the weight of the surface-dried specimens were measured. The changes in weight of the specimens were recorded at the time intervals to study the moisture absorption of the specimens.

The temperature of water in the containers were also measured three times at the time intervals. As the lab was air conditioned, the temperature was almost constant with an average of 21.0 °C and standard deviation of 0.2 °C. This is why the room temperature condition is referred as 20 °C. For the high heat of 60 °C, the containers were kept in ovens with accurate temperature control system. The average temperature of the solutions in the ovens was 61.3 °C with standard deviation of 0.6 °C. As the containers were sealed properly, no evaporation was observed, even at 60 °C. At each time interval taking the specimens out of the water solution, the pH level of the solution was also measured three times using a digital pH meter. The average pH of the solution at 20 °C during the period of 63 days was 9.7 with standard deviation of 0.02. The average pH of the solution at 60 °C during the same period of 63 days was 11.4 with standard deviation of 0.03. It should be mentioned that the initial pH of solutions was about 7, however the solutions gained their alkalinity from concrete. Overall, the average pH level of the solutions at 60 °C was observed 17% higher the solutions at 20 °C, due to more alkaline leach from the concrete specimens into the solutions.

As presented in Table 1, five specimens were exposed to 25 cycles of freeze/thaw using a freeze/thaw cabinet. The minimum temperature was -18 °C and maximum was 4 °C with a duration of 4 hours for each cycle. A 30 minute transition was set between the maximum and minimum temperatures. After the completion of the freeze/thaw cycles, the specimens were post-conditioned as same as the specimens immersed in water and were tested under three-point bending.

2.5. Test Setup

After the end of each environmental conditioning and before the mechanical testing, the specimens were post-conditioned for a period of 24 hours in an air circulating oven at a temperature of 50 °C to make sure all specimens have the same moisture content at the time of the mechanical testing. Then, the post-conditioned specimens were removed from the oven and were cooled down to the room temperature for a period of at least 5 hours prior to the mechanical testing. A 30 kN universal testing machine was used to perform the three-point bending test as shown in Fig. 3. The tests were displacement controlled with a rate of 0.5 mm/min. The load was measured by the machine's load cell and the deflection at mid-span was collected based on the cross-head displacement of the frame as no displacement gauge was available to the authors at the time of the research. The beam specimens were tested with a simply supported span of 300 mm with 50 mm overhang at each end up to the failure.

3. RESULTS AND DISCUSSIONS

This section provides the results of the experimental work and discussions on failure modes, load-deflection behavior, ductility, effect of aging, weight gain, and peak load retention. Table 3 summarizes the test results including the peak load, ultimate deflection, pseudo-ductility ratio, and weight gain. It provides the average value (AVG), standard deviation (SD), and coefficient of variation (COV) of each parameter.

3.1. Failure Modes

As shown in Fig. 4, typical failure mode was a debonding of the FRP from the concrete at the interface (i.e. adhesive failure), not in concrete (i.e. cohesive failure). It should be highlighted that having the adhesive failure was the target of the research. However, a few partial flax FRP rupture in the bonding

region was observed as shown in Fig. 4(a). Overall, slightly before the brittle failure, some noises and minor cracks at the vertical sides of the concrete specimens along the bonding surface of FRP and concrete were observed. It was also observed that the debonding failure occurred randomly at the left or right sides of the saw cut. For some specimens, a triangle-shape concrete at the corner of the FRP and the saw cut was left attached to the FRP as shown in Fig. 4(a) and 4(b). For the control specimens, some mortar remained locally adhered to the FRP, however for the aged specimens, as shown in Fig. 4(c) and 4(d), less mortar was left on FRP after the adhesive failure, which demonstrates the influence of the ageing process. For the specimens aged with 25 cycles of freeze/thaw, a cohesive failure mode occurred, as shown in Fig. 4(e) and 4(f). It means the freeze/thaw cycles affected the concrete rather than the adhesive. It should be mentioned that a set of specimens (5 specimens with bonded flax and 5 with bonded glass FRPs) were aged with 50 cycles of freeze/thaw, the results was complete cohesive failure at the end of the aging process without any mechanical test, where the failure surface was completely in concrete rather than in adhesive. As the mechanical test was not possible on the specimens with 50 cycles of freeze/thaw, those 10 specimens were not included in the test matrix of this study.

3.2. Load-Deflection Behavior

Figs. 5(a) and 5(b) show the typical load-deflection behavior of the specimens with bonded flax and glass FRPs, respectively. As shown, only one curve (the one that was the closest curve to the average) out of the five identical specimens was selected and presented in the figures. Overall, the figures show a linear initial branch to a certain point, where an initial debonding alters it to a secondary branch towards a complete debonding of the FRP from the concrete. The specimens with bonded flax FRP

exhibit a significant longer secondary branch than the ones with bonded glass FRPs. In order to quantify the phenomenon, a pseudo-ductility ratio (μ) is defined as follows:

$$\mu = \frac{\delta_u}{\delta_i} \quad (1)$$

where δ_i is the deflection at the initial debonding and δ_u is the deflection at the ultimate deflection. The pseudo-ductility ratio of all five identical specimens of each group accompanied by the peak load and the ultimate deflection of the specimens were calculated and the average, standard deviation, and coefficient of variation values are presented in Table 3. The following sections provide a detailed discussion about the effect of each environmental condition on the load-deflection behavior of the test specimens.

3.2.1. Control Specimens

Five specimens with bonded flax FRP (F-AD-T20-D0) and five specimens with bonded glass FRP (G-AD-T20-D0) were tested as control specimens without any aging. The control specimens were tested at day 0, when the aging process was started for the rest of the specimens. As shown in Fig. 5(a), the control specimens with bonded flax FRP have a linear behavior up to a certain point, where an initial debonding begins and extends with a flat secondary branch, then the complete debonding failure occurs. As shown in Fig. 5(b), the control specimens with bonded glass FRP show similar linear behavior with slightly larger initial stiffness up to the failure with a smaller pseudo-ductility ratio (see Table 3). The slight larger initial stiffness can be explained by larger stiffness of glass FRP compared to that of flax FRP. The larger pseudo-ductility of control specimens with bonded flax FRP might be related to the nonlinear behavior of flax FRP compared to the linear behavior of glass FRPs (see Fig. 1). The nonlinear behavior of flax FRP and its lower secant modulus at higher stresses can cause a gradual transformation of tensile stress from the FRP to the shear stress at the interface of the

concrete and the FRP, which can result in a more gradual debonding compared to the sudden debonding of the specimens with bonded glass FRP. In order to quantify this phenomenon, a more in-depth research with precise strain measurement of FRPs is needed. It should be noted that at the time of the research, no strain measuring system was available to the authors. In fact, the initial focus of the research was on the overall load capacity of the concrete beams with bonded flax FRP and the deterioration of the capacity after aging with heat and water solution compared to the ones with bonded glass FRP. In Section 4, a cross-sectional analytical model is presented to compute the FRP strain.

3.2.2. Effect of Dry Heat

This section focuses on the effect of dry heat (i.e. air dry condition) on the load-deflection behavior of the specimens exposed to a constant temperature of 60 °C. After the end of the exposure, the specimens were cooled down to the room temperature for at least 5 hours, then they were tested with similar test setup of the control specimens. Fig. 5(a) indicates that the 60 °C dry heat condition for 63 days increased the peak load and altered the flat secondary branch of the control specimens with bonded flax FRP to a shallow ascending branch. This can be explained by the post-curing of the resin at high temperature and an increase of the cross-links density of the bonding polymer, which is reflected in an increase of strength and stiffness of the FRP. As presented in Fig. 5(b), the specimens with bonded glass FRP aged in 60 °C dry heat for 63 days exhibit similar linear behavior with slightly larger stiffness up to a point where the debonding occurs suddenly. The load capacity is larger than the control specimens, however the coefficient of variation of test results is higher (see Table 3). As shown in Fig. 5, it is also observed that the peak load of both specimens bonded with flax and glass FRPs kept dry at the room temperature (20 °C) for 63 days is slightly less than that of the control

specimens. This could be related to the nature of concrete absorbing the humidity of environment affecting the bond strength. This is important regarding the effect of both heat and water immersion, which is discussed in the following sections.

3.2.3. Effect of Water Immersion in Room Temperature

This section presents the load-deflection behavior of the specimens aged in water solution in room temperature (20 °C). After aging for 21, 42, and 63 days, the specimens were tested with a procedure similar to the control specimens. As shown in Fig. 5(a) using the dashed lines, after the initial debonding of flax FRPs, the curves extend with a deep descending branch down to the complete bond failure. The descending branches differentiate the behavior of the specimens with respect to the control specimens with an almost flat secondary branch and the specimens kept in room temperature dry condition with a shallow secondary branch. Moreover, the moisture decreases the peak load of the specimens compared to the control specimens and the specimens kept in dry condition. It also can be concluded that increasing the duration of immersion into 20 °C water decreases the peak load, slightly. As shown in Fig. 5(b), the specimens with bonded glass FRP aged in 20 °C water were experienced very little peak load reduction compared to their control specimens. Overall, the specimens with bonded flax FRP were affected much more than their counterparts with glass FRP by the immersion into water in room temperature.

3.2.4. Effect of Water Immersion in High Heat

The load-deflection behavior of the specimens after 21-, 42-, and 63-day immersion in 60 °C water solution is discussed in this section. As shown in Fig. 5(a), after the initial debonding, the curve extends with a shallow descending branch down to the complete bond failure. The descending

branches differentiate the behavior of the specimens with respect to the control specimens and the specimens aged in dry heat. Overall, it can be observed that increasing the temperature along with the duration of immersion into 60 °C water decreases the peak load. However, the specimens are slightly stronger than their counterparts immersed in water in room temperature. In order to have a fare comparison, the specimens should be compared to their counterparts aged at the same temperature, as high heat increases the strength and stiffness of the bonding polymer. This is discussed in Section 3.3. As shown in Fig. 5(b), the specimens with bonded glass FRP aged in 60 °C water for 63 days were experienced more peak load reduction compared to the specimens with shorter exposures.

3.2.5. Effect of Freeze/Thaw Cycles

This section presents the load-deflection behavior of the specimens exposed to 25 cycles of freeze/thaw with a minimum temperature of -18 °C and maximum temperature of 4 °C with a duration of 4 hours per cycle. As shown in Fig. 5(a), the specimens with bonded flax FRP have a shallow linear behavior up to a point where a cohesive debonding failure occurs suddenly. A comparison to the control specimens demonstrates that cohesive debonding is a premature failure as the concrete was affected significantly by the freeze/thaw cycles, which prevented an adhesive failure at the interface. The specimens with bonded glass FRP demonstrate similar behavior with higher peak load. It should be noted that at 50 cycles all 10 specimens lost their FRP at the end of freeze/thaw cycles, so they were not tested under bending and were not included in the test matrix of this study. It is recommended to use a lower number of freeze/thaw cycles to obtain a critical number of cycles required for switching the failure mode from an adhesive bond failure to a cohesive bond failure.

3.3. Peak Load and Peak Load Retention

In order to have a more in-depth evaluation about the effect of the environmental conditions on the specimens, Figs. 6(a) and 6(b) presents the peak load of the specimens with bonded flax and glass FRPs, respectively. The variation bars show a standard deviation above and below the average value. The figures show that the peak load of the control specimens with bonded flax FRP is 20% weaker than their counterparts with bonded glass FRP. The figures also indicate that there is a peak load reduction by immersing the specimens with bonded flax FRP in water with respect to the control specimen tested at the day 0. The specimens with bonded glass FRP do not experience similar reduction. Moreover, the figures show that the specimens kept in 60 °C dry heat condition are stronger than their control specimens. That means the reference specimens for the specimens aged in 60 °C water should be their counterparts kept in 60 °C dry heat condition. For better comparison, a peak load retention percentage is calculated for each specimen based on ACI 440.9R-15 [30]. The peak load retention of each specimen is calculated as follows:

$$R_P = \frac{P_2}{P_1} \times 100 \tag{2}$$

where R_P is the peak load retention in percent; P_1 is the average peak load of control specimens; and P_2 is the average peak load of aged specimens. Using Eq. (2), the peak load retention of the specimens aged in 20 and 60 °C water for 63 days is obtained 75% and 85% with respect to the control specimens, respectively. That indicates that the specimens with bonded flax FRPs aged in 60 °C water are 10% stronger than their counterparts aged in 20 °C water. The result seems in contradiction with the common belief about accelerated aging in water at high temperature. As mentioned earlier, the authors believe that the effect of resin curing at high temperature should be also considered. That is why a set of specimens was kept in 60 °C dry heat condition to understand better the effect of both heat and moisture. The results show a 5% reduction at 20 °C and 16% increase in peak load with

respect to that of the control specimens. By comparing the specimens with bonded flax FRPs aged for 63 days in water at 20 and 60 °C with respect to that of their counterpart in dry heat condition, the peak load retentions are resulted in 77% and 72%, respectively. For the specimens with bonded glass FRP, comparing the peak load of the specimens aged for 63 days in water at 20 and 60 °C with respect to that of their counterparts in dry condition, the peak load retentions are resulted in 104% and 80%, respectively. Overall, after 63 days immersing in 60 °C water, the peak load retention of the specimens with bonded flax and glass FRPs was 72% and 80% with respect to their counterpart specimens kept in 60 °C dry condition, respectively.

3.4. Weight Gain

In this section, the weight gain of the specimens is compared in order to understand the difference in the water absorption. This can help to understand the difference in long-term bond properties of the specimens. When the specimens were placed in water for different durations there was usually a weight gain due to the water absorption by both concrete and FRP materials. It should be noted that the weight gain is mainly due to water absorption of concrete, however the FRP has some effects. The weight gain can be calculated based on the oven dry weight and saturated surface dry weight of each specimen as follows:

$$M_t = \frac{W_t - W_d}{W_d} \times 100 \quad (3)$$

where M_t is the percentage of weight gain at the time t, W_d is the weight of the dry specimen at time t=0 and W_t is the weight of the saturated surface dry specimen at time t. As shown Table 3, it can be seen that the effect of temperature on the weight gain of both flax and glass FRP bonded specimens had the same trend, however the weight gain in glass the specimens with bonded glass FRP is lower than the ones with bonded flax FRP. Overall, the average weight gain of specimens with bonded flax

and glass FRPs were 2.8% and 2.4%, respectively. This is compatible with the hydrophilic nature of natural fibers and high absorption properties of flax FRPs as reported by Hristozov et al. [35].

3.5. Statistical Evaluations

In order to identify parameters with significant effect on the test specimen, an analysis of variance (ANOVA) is performed. ANOVA allows a comparison of the variance caused by the between-groups variability (Mean square effect or MS_{effect}) with the within-group variability (Mean square error or MS_{error}) by means of the F-test. The analysis results are presented in an F-value as follows:

$$F = \frac{MS_{effect}}{MS_{error}} \tag{4}$$

The analysis tests whether the F-value is significantly greater than a critical value F_{crit}, extracted from the distribution of statistical tables based on the number of degrees of freedom. A test result (calculated from the null hypothesis and the sample) is called statistically significant if it is deemed unlikely to have occurred by chance, assuming the truth of the null hypothesis. A statistically significant result justifies the rejection of the null hypothesis. In this study, a one-way ANOVA using a confidence level of 95% (significance level of 0.05) is performed.

In terms of the weight gain of the specimens, three parameters, namely, the type of fibers, the temperature, and the exposure duration are considered, separately. The result of the analysis is summarized in Table 4. Considering the type of fibers, the ANOVA analysis shows that the results are significant at the 5% significance level ($F>F_{crit}$), which rejects the null hypothesis, concluding that there is strong evidence that the weight gain between concrete specimens with bonded flax and glass FRPs differ significantly. As presented in Table 4, the effect of the temperature and exposure duration on the weight gain are considered non-significant since $F<F_{crit}$. It also indicates that the

duration of aging from 21 to 63 days and temperature have non-significant effect on the weight gain of both series of specimens.

In terms of the peak load, the ANOVA analysis indicates that the peak load of specimens with bonded flax FRP is significantly less than that of glass FRPs since $F>F_{crit}$ (see Table 4). This can be explained by the permeable nature of flax fibres compared to glass fibers as it can create more moisture path into the polymer leading to higher moisture absorption and consequently more deterioration [35]. In order to have a better understanding of the phenomenon, more research is needed to study the effect of different natural fibers and resins on the durability of the FRP-concrete bond. As shown in Table 4, the ANOVA analysis also indicates that the duration of aging in water has significant effect on the peak load of the specimens with bonded flax FRPs, however it has non-significant effect on the specimens with bonded glass FRPs. It also shows that the duration of aging from 21 to 63 days has non-significant effect on the peak load of both series of specimens considered in this study.

4. ANALYTICAL STUDY

This section presents a cross-sectional analytical study to compute the resultant tensile force in the FRP strip and its corresponding tensile strain as well as the bond strength between the concrete and the FRP, particularly at the peak load. The analytical model considers the nonlinear behavior of concrete in compression and the nonlinear behavior of FRP in tension (for the case flax FRP). As shown in Fig. 7, the strain profile is assumed linear and the tensile strength of concrete is ignored. The model does not consider the slip between the concrete and the FRP after the initial bonding. Thus, its output for the specimens with a peak load way beyond of the initial debonding could be approximate. As there is no strain measurement in the current experimental study, the authors are not

able to validate the accuracy of the model. As shown in Fig. 7, the neutral axis depth (c) is measured from the extreme concrete compression fiber. Thus, strains of FRP (ε_f) and concrete (ε_c) are proportional with the maximum concrete strain ε_{cm} in compression and the curvature ψ. As there is no transverse FRP for confinement and concrete does not reach to its crushing point, the compressive behavior of concrete can be adequately described by the parabolic formula. As shown in Fig. 7, the compressive stress (f_c) at distance y from the neutral axis, corresponding to a strain ε_c, is given by [40]:

$$f_c = f'_c\left[2\frac{\varepsilon_c}{\varepsilon'_c} - \left(\frac{\varepsilon_c}{\varepsilon'_c}\right)^2\right] \quad (5)$$

where f'_c is the concrete strength in compression and ε'_c is its corresponding strain. The corresponding strain and the elastic modulus (E_c) are determined as $\varepsilon'_c=1.7f'_c/E_c$ and $E_c=4700(f'_c)^{0.5}$ (in MPa); respectively. The behavior of glass FRPs is assumed linear elastic up to the tensile rupture stress as presented in Fig. 1. The behavior of flax FRPs is assumed bilinear with a kinking point at strain 0.0025 mm/mm and a secondary stiffness equal to 2/3 of the initial stiffness up to the tensile rupture stress as presented in Fig. 1. Based on Hristozov et al. [35], the aging process does not affect the modulus of flax and glass FRPs, significantly. As a results, the stress-strain curve of flax and glass FRPs aged in this study are assumed as same as their control counterparts. In fact, the aging process only affects the rupture point of FRPs. As bond failure controls the failure of the beam specimens with bonded FRPs, the rupture points of the FRPs have no effect on the current analytical model. Based on Fig. 7, the strain ε_c at any concrete compression fiber is evaluated as $\varepsilon_c=\psi.y$ and strain ε_{cm} at extreme concrete compression fiber (i.e. at $y=c$) is evaluated as $\varepsilon_{cm}=\psi.c$. Thus, the resultant force C_c corresponding to the compressive concrete and its moment M_c about the neutral axis can be expressed as follow:

$$C_c = b\int_0^c f_c dy \tag{6}$$

$$M_c = b\int_0^c f_c y dy \tag{7}$$

For FRP, strain ε_f is evaluated as $\varepsilon_f=\psi(d_f-c)$. Thus, using the stress-strain behavior of the FRP (Fig. 1), the tensile force of FRP per unit width (f_f) and the resultant force $T_f=b.\ f_f$ can be computed. To this end, the internal forces have been expressed in terms of two main parameters, namely; the curvature ψ and neutral axis depth c. By applying static equilibrium conditions, considering internal and external forces (Fig. 7), the following two equations are derived:

$$C_c = T_f \tag{8}$$

$$M_c + T_f\left(d_f - c\right) = PL/4 \tag{9}$$

where P is the average peak load of each five identical experimental specimens. Eqs. (8) and (9) are sufficient to obtain the two unknown parameters (i.e. curvature ψ and neutral axis depth c), using a conventional computer program. Then, the tensile strain of FRP (ε_f) at the peak load and the corresponding resultant force (T_f) are computed. The bond strength ($\tau_u=T_f/A$) between the concrete and the FRP is also computed, where A is the bonding area of the FRP and concrete at either side of the mid-span. The procedure is completed for each group of the experimental specimens at the average peak load and the results are presented in Table 5. In order to provide a reasonable comparison of the FRP systems and bond strength, the bond strength values are normalized ($\bar{\tau}_u$) based on the area (A_f) and modulus (E_f) of each FRP as follows:

$$\bar{\tau}_u = \frac{\tau_u}{A_f E_f} \tag{10}$$

Using the analytical model, the FRP force (T_f), the FRP strain (ε_f), the bond strength (τ_u), and the normalized bond strength ($\bar{\tau}_u$) were computed at the average peak load of each group of test

specimens. The results are presented in Table 5. It shows that there is a difference between the bond strength of the specimens with bonded flax and glass FRPs. An ANOVA analysis shows that the difference is significant (see Table 4). However, the same ANOVA analysis on the normalized bond strength shows that there no significant difference between the specimens with bonded flax and glass FRP $F<F_{crit}$ (see Table 4).

The bond strength retention (R_r) of each group of specimens was also calculated based on the bond strength computed using the analytical method. The results are presented in Table 5 with respect to the control specimens tested at day 0 and at day 63 (T= 20 and 60 °C). The results indicate that the bond strength retentions of the specimens with bonded flax and glass FRPs immersed in 60 °C water for 63 days is 69% and 79% of their counterparts kept in dry heat condition, respectively.

Based on ACI 440.2R-08 [41], a failure controlled by FRP debonding may occur away from where an externally-bonded FRP terminates due to the intermediate crack-induced (IC) debonding failure. The tensile strain in FRP at which the IC debonding may occur (ε_{fd}) is defined as follows:

$$\varepsilon_{fd} = 0.41\sqrt{\frac{f'_c}{nE_f t_f}} \tag{11}$$

where E_f and t_f are the elastic modulus and thickness of a single ply of the FRP laminate, n is the number of plies, and f'_c is the compressive strength of concrete. Using Eq. (11), the IC debonding strain of the flax and glass FRPs used in this study is computed as 0.0194 and 0.0172 mm/mm, respectively. The average tensile rupture strain of the flax and glass FRPs are 0.0131 and 0.0254 mm/mm as shown in Fig. 1. It means the specimens bonded with flax FRP are not vulnerable to the IC debonding (as $\varepsilon_{fd} = 0.0194 > \varepsilon_{fu} = 0.0131$), however the IC debonding can control the failure of the specimens with bonded glass FRP (as $\varepsilon_{fd} = 0.0172 < \varepsilon_{fu} = 0.0254$). As presented in Table 5, the maximum level of strain in flax and glass FRPs bonded to concrete specimens is 0.0102 and 0.0073 mm/mm, which are less than the critical values of 0.0131 and 0.0172 mm/mm, respectively. Thus,

the IC debonding did not control the failure of the specimens. In fact, the length of the bonded FRPs were initially designed short enough to keep the level of FRP strain lower than the critical values ensuring an adhesive bond failure controls the behavior of the specimens, rather than the FRP rupture/IC debonding/concrete crushing failures.

5. CONCLUSION

In this study, durability tests were conducted in order to investigate the long-term behavior of externally bonded natural and synthetic FRPs to concrete beam specimens. A total of 100 plain concrete beams were prepared and bonded with flax and glass FRPs. The test parameters were fiber type (flax vs. glass fibers), environmental aging condition (dry heat, immersed in water, and freeze/thaw), exposure duration (21, 42, and 63 days), and temperature during the exposure (20 and 60 °C). The specimens aged in the environmental conditions were tested under three-point bending and compared to control specimens. An analytical study also presented to compute the tensile strain and bond strength of the specimens. The following conclusions can be drawn from the study:

- Typical failure mode the specimens was a brittle debonding of the FRP from the concrete at the interface (i.e. adhesive failure). For the specimens aged with 25 cycles of freeze/thaw, the typical failure mode was a cohesive debonding, where the failure surface passed through the concrete.
- The typical load-deflection behavior of control specimens was linear and followed by a flat secondary branch after the initial debonding. The specimens with bonded glass FRP showed a secondary branch much shorter than the specimens with bonded flax FRP. The peak load of the control specimens with bonded flax FRP was 20% weaker than their counterparts with glass FRP. A one-way ANOVA analysis showed that the type of fibers has a significant effect on the peak load.

- Keeping the specimens in a dry condition at room temperature (i.e., 20 °C) reduced slightly the peak load, however dry heat condition (i.e., 60 °C) significantly enhanced the peak load due to increasing of the cross-links density of the bonding polymer. This was resulted in a shallow ascending secondary branch for flax bonded specimens exposed to dry heat condition.
- For the specimens immersed in water at room temperature, the specimens with bonded flax FRP were affected much more than their counterparts with glass FRP. For the specimens with bonded flax FRP, the secondary branch was shortened with a descending trend as the duration of the immersion increased. For the specimens with bonded glass FRP, there was no significant change.
- For the specimens immersed in water at high heat (i.e., 60 °C), longer duration of immersion did have a significant deterioration effect on the peak load. Also, increasing the temperature from 20 to 60 °C along with the duration of immersion decreased the peak load. After 63-day immersion in 60 °C water, the peak load retention of the specimens with bonded flax and glass FRPs was 72% and 80% with respect to their counterpart specimens kept in 60 °C dry condition, respectively.
- Using a cross-sectional analytical model, the tensile force, tensile strain, and bond stress of the test specimens at peak load were computed. The bond strengths were normalized by the area and modulus of the FRPs. It was shown that there was a significant difference between the bond strength of the specimens with bonded flax and glass FRPs. However, there was non-significant difference between the normalized bond strengths.

ACKNOWLEDGEMENTS

The authors acknowledge the financial support of Penn State Harrisburg and Dalhousie University.

REFERENCES

[1] Bakis C, Bank LC, Brown V, Cosenza E, Davalos JF, Lesko JJ, Machida A, Rizkalla SH, Triantafillou TC. Fiber-reinforced polymer composites for construction-state-of-the-art review. Journal of Composites for Construction. 2002;6(2):73-87.

[2] Teng JG, Chen JF, Smith ST, Lam L. Behaviour and strength of FRP-strengthened RC structures: a state-of-the-art review. Proceedings of the institution of civil engineers-structures and buildings. 2003;156(1):51-62.

[3] Pickering SJ. Recycling technologies for thermoset composite materials—current status. Composites Part A: Applied Science and Manufacturing. 2006;37(8):1206-15.

[4] Yazdanbakhsh A, Bank LC. A Critical Review of Research on Reuse of Mechanically Recycled FRP Production and End-of-Life Waste for Construction. Polymers. 2014;6(6):1810-26.

[5] Wambua P, Ivens J, Verpoest I. Natural fibres: can they replace glass in fibre reinforced plastics?. Composites Science and Technology, 2003;63(9):1259-1264.

[6] Mohanty AK, Misra M, Drzal LT. Sustainable bio-composites from renewable resources: opportunities and challenges in the green materials world. Journal of Polymers and the Environment, 2002;10(1-2):19-26.

[7] Herrera-Franco P, Valadez-Gonzalez A. A study of the mechanical properties of short natural-fibre reinforced composites. Composites Part B: Engineering, 2005;36(8):597-608.

[8] Ku H, Wang H, Pattarachaiyakoop N, Trada M. A review on the tensile properties of natural fibre reinforced polymer composites. Composites Part B: Engineering, 2011;42(4):856-873.

[9] Faruk O, Bledzki AK, Fink HP, Sain M. Progress report on natural fibre reinforced composites. Macromolecular Materials and Engineering, 2014;299(1):9-26.

[10] Kabir MM, Wang H, Lau KT, Cardona F. Chemical treatments on plant-based natural fibre reinforced polymer composites: An overview. Composites Part B: Engineering. 2012 Oct 31;43(7):2883-92.

[11] Yan L, Chouw N, Jayaraman K. Flax fibre and its composites–a review. Composites Part B: Engineering, 2014;56:296-317.

[12] Shah DU, Schubel PJ, Clifford MJ. Can flax replace E-glass in structural composites? A small wind turbine blade case study. Composites Part B: Engineering, 2013;52: 172-181.

[13] Di Bella, G, Fiore V, Valenza A. Effect of areal weight and chemical treatment on the mechanical properties of bidirectional flax fabrics reinforced composites," Materials & Design, 2010;31(9):4098-4103.

[14] Yan L, Chouw N, Yuan X. Improving the mechanical properties of natural fibre fabric reinforced epoxy composites by alkali treatment. Journal of Reinforced Plastics and Composites, 2012;31(6):425-437.

[15] Wang W, Sain M, Cooper PA. Study of moisture absorption in natural fiber plastic composites. Composites Science and Technology. 2006;66(3):379-86.

[16] Thwe MM, and Liao K. Durability of bamboo-glass fibre reinforced polymer matrix hybrid composites, Composites Science and Technology, 2003;63:375-387.

[17] Xie Y, Hill CA, Xiao Z, Militz H, Mai C. Silane coupling agents used for natural fibre/polymer composites: A review. Composites Part A: Applied Science and Manufacturing, 2010;41(7):806-819.

[18] Thwe MM, Liao K. Environmental effects on bamboo-glass/polypropylene hybrid composites. Journal of Materials Science, 2003;38(2):363-376.

[19] Bank LC, Gentry TR, Barkatt A. Accelerated test methods to determine the long-term behavior of FRP composite structures: environmental effects. Journal of Reinforced Plastics and Composites. 1995;14(6):559-87.

[20] Toutanji HA, Gomez W. Durability characteristics of concrete beams externally bonded with FRP composite sheets. Cement and Concrete Composites. 1997;19(4):351-8.

[21] Green MF, Bisby LA, Beaudoin Y, Labossière P. Effect of freeze-thaw cycles on the bond durability between fibre reinforced polymer plate reinforcement and concrete. Canadian Journal of Civil Engineering. 2000;27(5):949-59.

[22] Karbhari VM, Chin J, Hunston D, Benmokrane B, Juska T, Morgan R, Lesko JJ, Sorathia U, Reynaud D. Durability gap analysis for fiber-reinforced polymer composites in civil infrastructure. Journal of Composites for Construction. 2003;7(3):238-47.

[23] Jia J, Boothby TE, Bakis CE, Brown TL. Durability evaluation of glass fiber reinforced-polymer-concrete bonded interfaces. Journal of Composites for construction. 2005;9(4):348-59.

[24] Abanilla MA, Li Y, Karbhari VM. Durability characterization of wet layup graphite/epoxy composites used in external strengthening. Composites Part B: Engineering. 2006;37(2):200-12.

[25] Myers JJ. Durability of external fiber-reinforced polymer strengthening systems. In: Karbhari VM, editor. Durability of composites for civil structural applications. Cambridge, UK: Woodhead Publishing Limited; 2007. p. 247–83.

[26] Tuakta C, Büyüköztürk O. Deterioration of FRP/concrete bond system under variable moisture conditions quantified by fracture mechanics. Composites Part B: Engineering. 2011;42(2):145-54.

[27] Cromwell JR, Harries KA, Shahrooz BM. Environmental durability of externally bonded FRP materials intended for repair of concrete structures. Construction and Building Materials. 2011;25(5):2528-39.

[28] Tatar J, Hamilton HR. Bond durability factor for externally bonded CFRP systems in concrete structures. Journal of Composites for Construction. 2015;10:04015027.

[29] Sen R. Developments in the durability of FRP-concrete bond. Construction and Building Materials. 2015;78:112-25.

[30] ACI 440.9R-15. Guide to accelerated conditioning protocols for durability assessment of internal and external fiber-reinforced polymer (FRP) reinforcement. American Concrete Institute, Farmington Hills, MI, USA; 2015.

[31] Gartner A, Douglas EP, Dolan CW, Hamilton HR. Small beam bond test method for CFRP composites applied to concrete. Journal of Composites for Construction. 2010;15(1):52-61.

[32] Azwa ZN, Yousif BF, Manalo AC, Karunasena W. A review on the degradability of polymeric composites based on natural fibres. Materials & Design. 2013;47:424-42.

[33] de Andrade Silva F, Toledo Filho RD, de Almeida Melo Filho J, Fairbairn ED. Physical and mechanical properties of durable sisal fiber–cement composites. Construction and building materials. 2010;24(5):777-85.

[34] Dhakal HN, Zhang ZY, Richardson MO. Effect of water absorption on the mechanical properties of hemp fibre reinforced unsaturated polyester composites. Composites Science and Technology. 2007;67(7):1674-83.

[35] Hristozov D, Wroblewski L, Sadeghian P. Long-term tensile properties of natural fibre-reinforced polymer composites: comparison of flax and glass fibres. Composites Part B: Engineering. 2016;95:82-95.

[36] ACI 318-11. "Building code requirements for structural concrete." American Concrete Institute, Farmington Hills, MI, USA, 2011.

[37] Sadeghian P, Hristozov D, Wroblewski L. Experimental and analytical behavior of sandwich composite beams: Comparison of natural and synthetic materials. Journal of Sandwich Structures and Materials. 2016:1099636216649891.

[38] ASTM D7565/D7567M-10. "Standard Test Method for Determining Tensile Properties of Fiber Reinforced Polymer Matrix Composites Used for Strengthening of Civil Structures." American Society for Testing and Materials, West Conshohocken, PA, USA, 2010.

[39] ACI 440.2R. "Guide for the design and construction of externally bonded FRP systems for strengthening concrete structures." American Concrete Institute, Farmington, MI, USA, 2008.

[40] Collins MP, Mitchell D. Prestressed concrete structures. Englewood Cliffs, NJ: Prentice Hall; 1991.

[41] ACI 440.2R-08. "Guide for the design and construction of externally bonded FRP systems for strengthening concrete structures." American Concrete Institute, Farmington, MI, USA, 2008.

Table 1. Test matrix.

Exposure Duration (days)	Dry		Water		Freeze/Thaw
	T=20°C	T=60°C	T=20°C	T=60°C	25 Cycles
0	5	-	-	-	5
21	-	-	5	5	
42	-	-	5	5	
63	5	5	5	5	
Total	100 (50 flax and 50 glass) FRP bonded concrete beams				

Table 2. Concrete mix design for 1 m^3 of concrete.

Ingredients	Weight (kg)
Coarse Aggregate	1076
Fine Aggregate	700
Water	207
Cement	421

Table 3. Summary of experimental results.

#	Specimen ID	Peak load, P_{max}			Ultimate deflection, δ_u			Pseudo-ductility ratio, μ			Weight gain, W_t		
		AVG (kN)	SD (kN)	COV (%)	AVG (mm)	SD (mm)	COV (%)	AVG (-)	SD (-)	COV (%)	AVG (%)	SD (%)	COV (%)
1	F-AD-T20-D0	10.49	0.25	2.38	1.96	0.18	9.42	1.33	0.12	9.08	-	-	-
2	G-AD-T20-D0	13.15	1.00	7.57	2.11	0.14	6.83	1.10	0.03	2.80	-	-	-
3	F-W-T20-D21	7.92	0.77	9.66	1.38	0.25	18.36	1.28	0.17	13.64	2.92	0.26	8.93
4	G-W-T20-D21	12.55	1.21	9.60	1.93	0.22	11.48	1.09	0.04	3.46	2.42	0.45	18.62
5	F-W-T60-D21	9.14	0.57	6.26	1.49	0.23	15.11	1.22	0.12	9.96	2.24	0.37	16.34
6	G-W-T60-D21	12.43	0.63	5.03	1.75	0.16	9.21	1.07	0.05	4.47	2.29	0.22	9.78
7	F-W-T20-D42	8.11	0.31	3.88	1.40	0.21	15.14	1.26	0.12	9.91	2.73	0.61	22.17
8	G-W-T20-D42	12.63	1.66	13.10	2.09	0.38	17.98	1.12	0.10	9.06	2.42	0.21	8.87
9	F-W-T60-D42	8.86	0.79	8.97	1.73	0.29	16.51	1.34	0.19	14.00	2.73	0.27	9.76
10	G-W-T60-D42	14.10	0.65	4.60	2.13	0.14	6.48	1.05	0.00	0.25	2.04	0.17	8.55
11	F-W-T20-D63	7.72	0.55	7.19	1.26	0.19	15.02	1.23	0.15	12.02	3.06	0.35	11.58
12	G-W-T20-D63	13.39	1.07	7.99	2.09	0.22	10.39	1.15	0.12	10.02	2.04	0.32	15.57
13	F-W-T60-D63	8.76	0.65	7.40	1.57	0.23	14.33	1.28	0.11	8.97	2.79	0.75	26.83
14	G-W-T60-D63	11.80	0.83	7.00	1.81	0.08	4.29	1.13	0.06	5.44	2.35	0.32	13.46
15	F-AD-T20-D63	9.98	0.64	6.43	2.03	0.18	8.95	1.62	0.15	9.04	-	-	-
16	G-AD-T20-D63	12.83	0.58	4.54	1.92	0.46	23.98	1.10	0.06	5.80	-	-	-
17	F-AD-T60-D63	12.21	0.60	4.93	2.14	0.11	4.97	1.36	0.07	5.02	-	-	-
18	G-AD-T60-D63	14.78	2.64	17.85	2.24	0.46	20.50	1.13	0.06	5.51	-	-	-
19	F-FT-C25	5.55	1.25	22.51	1.24	0.21	16.92	1.13	0.10	8.46	-	-	-
20	G-FT-C25	7.70	0.62	8.03	1.47	0.25	17.13	1.01	0.00	0.44	-	-	-

Table 4. The results of one-way ANOVA F-test evaluations

Evaluated parameter	Range of data	Source of variation	F-value	F_{crit}	Significance
Weight gain	All specimens aged in water	Type of fibers (flax and glass fibers)	12.84	4.96	Significant
	Flax FRP-bonded specimens aged in water	Temperature (20 and 60 ºC)	2.55	7.71	Non-significant
	Glass FRP-bonded specimens aged in water	Temperature (20 and 60 ºC)	0.19	7.71	Non-significant
	Flax FRP-bonded specimens aged in water	Exposure duration (21, 42, and 63 days)	0.66	9.55	Non-significant
	Glass FRP-bonded specimens aged in water	Exposure duration (21, 42, and 63 days)	0.34	9.55	Non-significant
Peak load	All specimens aged in water and high heat	Type of fibers (flax and glass fibers)	7.43	4.49	Significant
	Flax FRP-bonded specimens aged in water	Temperature (20 and 60 ºC)	38.88	7.70	Significant
	Glass FRP-bonded specimens aged in water	Temperature (20 and 60 ºC)	0.01	7.71	Non-significant
	Flax FRP-bonded specimens aged in water	Exposure duration (21, 42, and 63 days)	0.09	9.55	Non-significant
	Glass FRP-bonded specimens aged in water	Exposure duration (21, 42, and 63 days)	0.58	9.55	Non-significant
Bond strength	All specimens	Type of fibers (flax and glass fibers)	20.71	4.41	Significant
Normalized bond strength	All specimens	Type of fibers (flax and glass fibers)	1.94	4.41	Non-significant

Table 5. Summary of analytical study.

#	Specimen ID	FRP force at peak load, T_f (kN)	FRP strain at peak load, ε_f (mm/mm)	Bond strength, τ_u (MPa)	Normalized bond strength, $\bar{\tau}_u$ (m^{-2})	Bond strength retention, R_τ (%)	
						WRT D63[a]	WRT D0[b]
1	F-AD-T20-D0	10.76	0.0086	1.43	0.66	106	100
2	G-AD-T20-D0	13.63	0.0065	1.82	0.65	103	100
3	F-W-T20-D21	8.12	0.0062	1.08	0.49	77	72
4	G-W-T20-D21	13.00	0.0062	1.73	0.62	98	95
5	F-W-T60-D21	9.37	0.0073	1.25	0.57	72	85
6	G-W-T60-D21	12.88	0.0061	1.72	0.61	84	94
7	F-W-T20-D42	8.31	0.0063	1.11	0.51	78	73
8	G-W-T20-D42	13.09	0.0062	1.75	0.62	98	95
9	F-W-T60-D42	9.08	0.0070	1.21	0.55	69	81
10	G-W-T60-D42	14.62	0.0070	1.95	0.70	96	108
11	F-W-T20-D63	7.91	0.0060	1.05	0.48	74	70
12	G-W-T20-D63	13.88	0.0066	1.85	0.66	105	102
13	F-W-T60-D63	8.98	0.0070	1.20	0.55	69	81
14	G-W-T60-D63	12.22	0.0058	1.63	0.58	79	89
15	F-AD-T20-D63	10.23	0.0081	1.36	0.62	100	94
16	G-AD-T20-D63	13.29	0.0063	1.77	0.63	100	97
17	F-AD-T60-D63	12.53	0.0102	1.67	0.76	100	119
18	G-AD-T60-D63	15.33	0.0073	2.04	0.73	100	112
19	F-FT-C25	5.69	0.0039	0.76	0.35	48	45
20	G-FT-C25	7.96	0.0038	1.06	0.38	60	58

[a] WRT D0: with respect to corresponding control specimen bonded with flax/glass FRP.
[b] WRT D63: with respect to corresponding specimen bonded with flax/glass FRP aged in 20/60 °C air dry condition for 63 days.

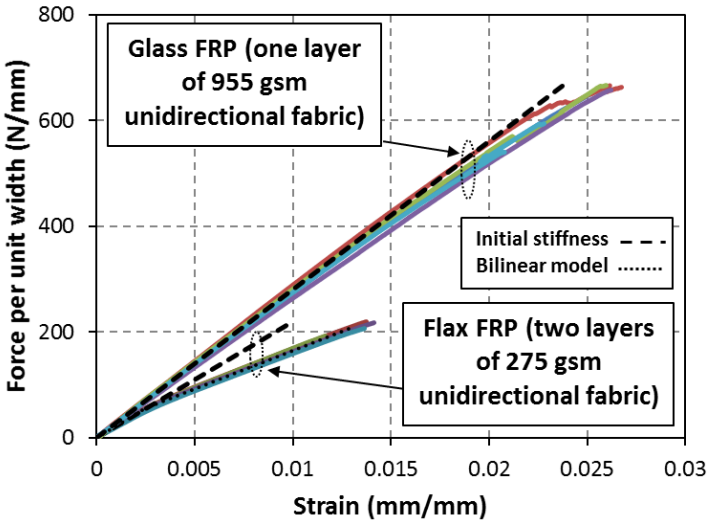

Figure 1. Tensile force per unit width versus strain curves of flax and glass FRPs.

Figure 2. Specimen preparation: (a) formwork; (b) surface preparation; (c); oven drying; and (d) applying FRP.

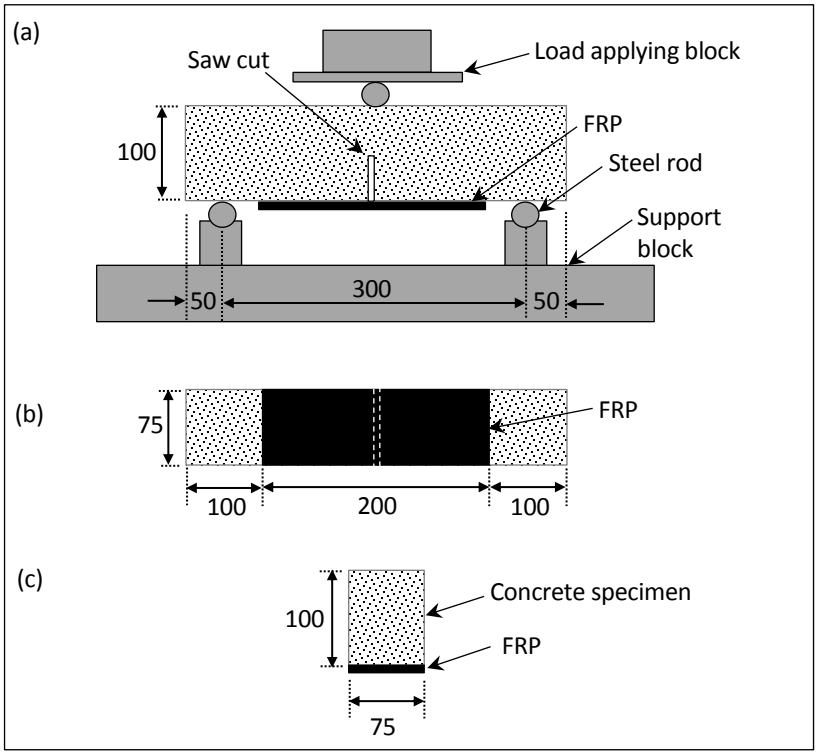

Figure 3. Test setup: (a) elevation view; (b) bottom view; and (c) cross-section (dimensions in mm).

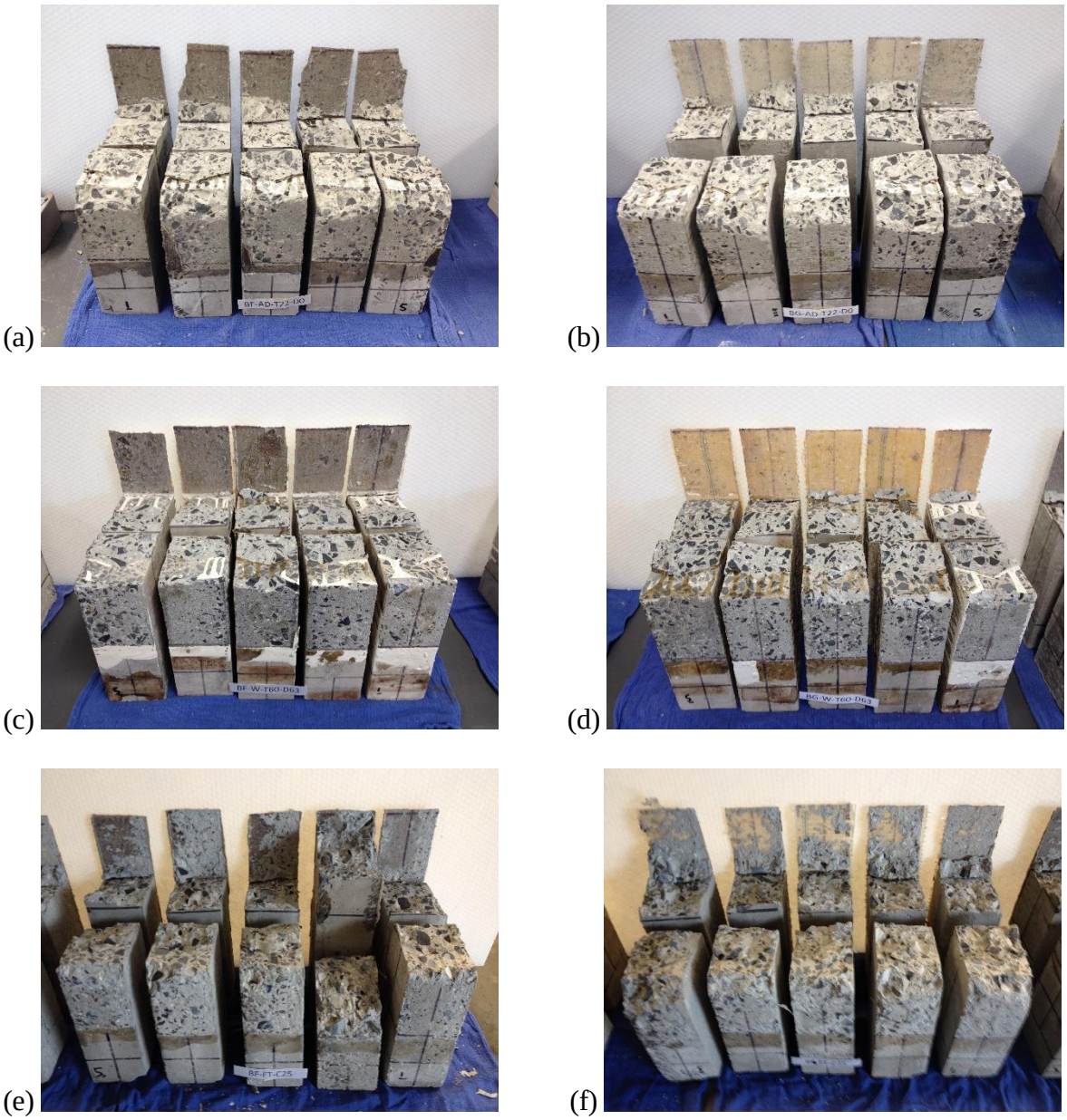

Figure 4. Failure mode of selected specimens: (a) F-AD-T20-D0 (Control); (b) G-AD-T20-D0 (Control); (c) F-W-T60-D63; (d) G-W-T60-D63; (e) F-FT-C25; and (f) G-FT-C25.

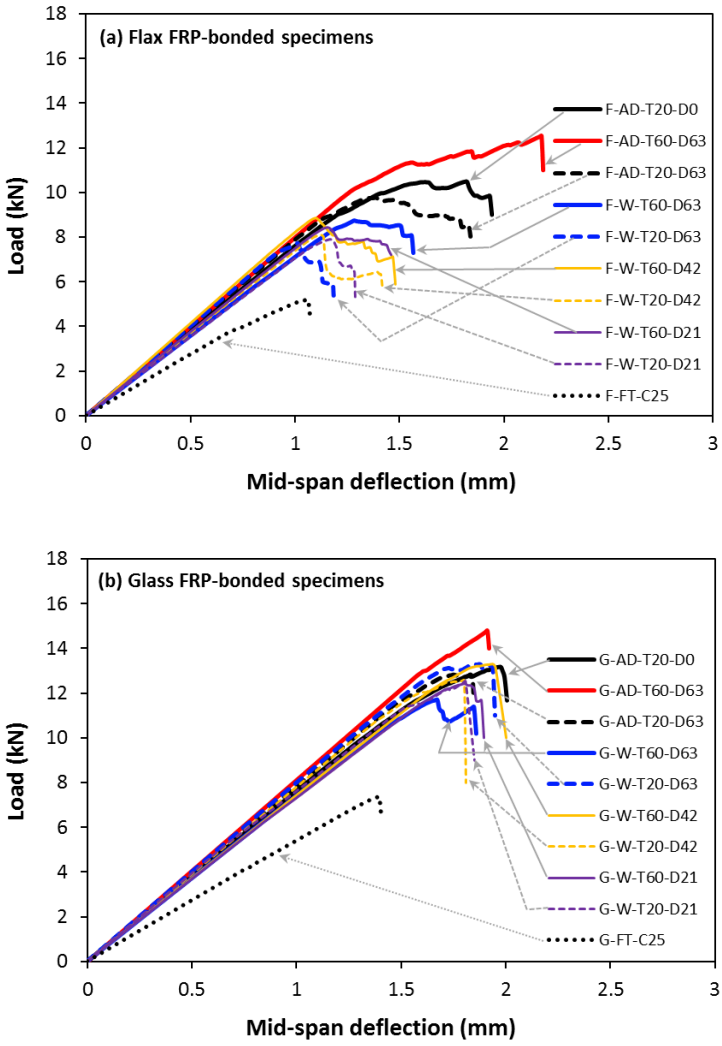

Figure 5. Load-deflection behavior of concrete beam specimens with bonded (a) flax and (b) glass FRPs.

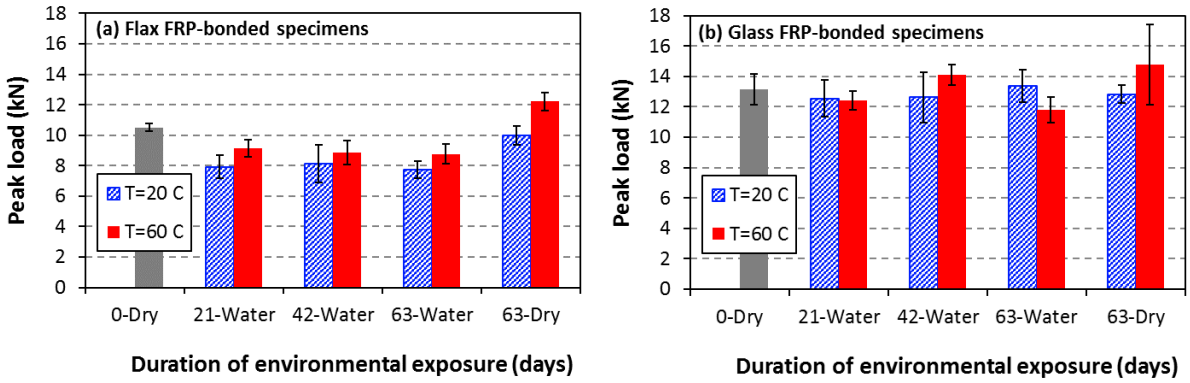

Figure 6. Variation in peak load of concrete beam specimens with bonded (a) flax and (b) glass FRPs.

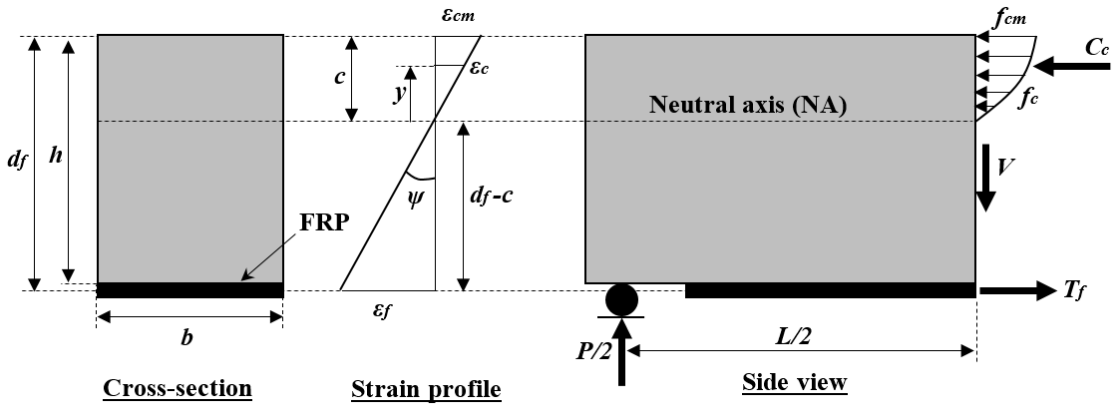

Figure 7. Mechanism of cross-sectional analytical model of concrete beam with bonded FRP.